Effects of Redox Response on Mouse Liver Cells Exposed to L-buthionine-Sulfoximine and Chitosan-Glutathione Nanoparticles

Sofia PinaOlmos[1], Patricia Ramirez-Noguera[1], J. H. Limon-Pacheco[2], Maria E. Gonsebatt-Bonaparte[2], Denise Lopez-Barrera[1], R. Diaz-Torres[1*]

[1]Department of Biological Sciences, Cellular Toxicology Laboratory, Multidisciplinary Research Unit, National Autonomous University of Mexico, State of Mexico, Mexico; [2]Department of Genomic Medicine and Environmental Toxicology, Biomedical Research Institute, National Autonomous University of Mexico, Mexico City, Mexico

ABSTRACT

There is interest in the use of nanomaterials as drug delivery vehicles or diagnostic systems, able to modulate cellular responses, which can be easily altered by many factors. Nanoparticles made of chitosan are considered suitable drug carriers due to their biocompatible properties; on the other hand, glutathione plays an essential role in the modulation of the redox balance into the cell. Glutathione is the major intracellular antioxidant, with many essential signaling functions. The depletion of this tripeptide activates several ways implied on the modulation of redox status that could lead to oxidative stress. Considering the activity of glutathione in various cellular events and the fact that its synthesis is only generated at the cytoplasmic level, the purpose of this work is to evaluate the ability of nanoparticles prepared with chitosan and glutathione to modulate redox cell responses on mouse liver cells (AML-12) exposed to L-Buthionine Sulfoximine (BSO) an inhibitor of the glutathione synthesis. Chitosan-glutathione nanoparticles were manufactured by ionic gelation then characterized by Transmission Electron Microscopy (TEM), Dynamic Light Scattering (DLS), and Z potential. The intracellular localization and cytotoxicity nanoparticles were evaluated by confocal microscopy and MTT assays, respectively. The ability to incorporate glutathione was determined through the intracellular GSH content assay, modulating the expression of the transcription factor Nrf2 and the antioxidant enzyme gene associated with glutathione Grx-1, was quantified using quantitative real-time PCR. The results showed nanoparticles into the cells and an increase of thiol content where nanoparticles were present, as well as an increase of the expression of Nrf2 and Grx-1 in a dose-dependent manner.

Keywords: Buthionine sulfoximine; Chitosan; Antioxidants; Drug carriers; Glutathione; Nanoparticles

INTRODUCTION

Glutathione (GSH) is considered the most abundant thiol-containing molecule in animal cells and plays several roles in cellular function, which has been extensively reviewed and includes drug detoxification [1], amino acid transport [2], antioxidant defense [3], redox signalling [4], storage of cysteine *via* the -glutamyl cycle [5], and regulation of growth and death[6]. GSH is synthesized in the cytoplasm of all animal cells from the amino acids L-glutamine, L-cysteine, and L-glycine in

two subsequent reactions catalyzed by γ-Glutamyl Cysteine Ligase (GCL) in the first-rate limiting step and GSH Synthase in the second step [7]. Buthionine sulfoximine binds to GCL, blocking GSH synthesis, leading to depletion of intracellular GSH [8–10], there are others ways to cause GSH depletion, they include drug metabolism like the case of acetaminophen an antipyretic drug mainly used around the world. When hepatic cells are exposed to acute concentrations of acetaminophen [11], GSH conjugation with the metabolites leads to a depletion of GSH reserves [12] and N-acetylcysteine administration has been shown a good

antidote [13,14]. In the last years, nanotechnology has facilitated the generation of new dosage forms more accurately and efficiently. One important application is the use of nanoparticles for the internalization of exogenous substances into the cell to modulate a biological responses; thiolate nanoparticles have been developed before by using glutathione [15–19], and others molecules with thiol groups [20–24], these nanoparticles made of chitosan have shown mucoadhesive properties with potential application as excipient for drug delivery systems and GSH delivery and as nanostructured systems they are useful in the treatment of breast cancer as a complement to radiotherapy [25-27]. Here, we explored the use of chitosan nanoparticles loaded with GSH to restore cellular GSH pool in cells treated with BSO. We present evidence that chitosan-GSH nanoparticles could compensate for the cellular viability after BSO treatment.

MATERIALS AND METHODS

Chemicals and reagents

Low Molecular Weight (LMW) Chitosan (CS) derived from crab shell, Fluorescein-5- isothiocyanate (FITC), Rhodamine 123, Reduced Glutathione (GSH), Sodium Tripolyphosphate (TPP), Glacial Acetic Acid, sodium hydroxide, Thiazolyl Blue Tetrazolium Bromide (MTT), N-Acetylcysteine (NAC), L-buthionine-sulfoximine and all other analytical grade chemicals were purchased from Sigma-Aldrich, St Louis MO, USA.

Preparation of chitosan-glutathione nanoparticles

Chitosan-glutathione (CS-GSH) nanoparticles were prepared by ionic gelation method [15,16] by using sodium Tripolyphosphate (TPP) anions with some modifications as follows. Briefly, LMW chitosan was dissolved in aqueous acetic acid (1% v/v) at the concentration of 0.3 % w/v. Chitosan solution was stirred at room temperature; then pH of the resulting solution was adjusted to 4.0 – 4.2 using sodium hydroxide solution 10 N. On the other hand, TPP was dissolved in ultrapure water at a concentration of 0.1 %. GSH was added to chitosan solution (0.01 g/mL) and stirred at room temperature for 60 minutes; after that, TPP (1:1 v/v) solution was quickly added to the CS-GSH solution. The reaction last 60 minutes more, and the resulting suspension was filtered through a 0.22 μm sterile syringe filter and stored at 4 °C.

Size measurement of CS-GSH nanoparticles

The average particle size, particle size distribution, and polydispersity index (PDI) of the nanoparticles were measured at 25°C by DLS on a high-performance particle sizer, Zeta sizer Nano (Malvern Instruments, MA, USA). Mean values were obtained from the analysis of three different batches, each of them measured three times.

Transmission Electronic Microscopy analysis (TEM)

TEM analyses evaluated the size and morphology of CS-GSH nanoparticles. Nanoparticle samples were prepared by putting the nanoparticles on a copper grid and left to dry at room temperature, then placed into the microscope by and analyzed by using a tungsten filament HV at 100 kV.

Determination of free thiol group content in nanoparticles

The number of free thiol groups in CS-GSH nanoparticles was measured spectrophotometrically using Elman's reagent (5,5'-dithio-bis-(2-nitrobenzoic acid) [17]. Briefly, the sample into the solution was diluted 1:10, and 10 μL were added to 190 μL of reaction buffer (1 M phosphate buffer pH 8.0 and of 6 mM Ellman's reagent) in a 96-well plate incubate for 15 minutes at 37°C. Then, the absorbance was measured at 450 nm with a microplate reader (MRC scientific instruments, London, UK). The total amount of sulfhydryl groups in CS-GSH nanoparticles was represented by the addition of reduced free thiol groups and oxidized thiol groups in the form of disulfide bonds.

Entrapment and loading efficiencies of CS-GSH nanoparticles

Entrapment Efficiencies (EE) and Loading Efficiencies (LE) of CS-GSH nanoparticles were determined by separation of supernatant from nanoparticle suspensions by ultracentrifugation of the nanoparticle suspension at 42000 x g for 60 min (Optima-XL-100K-Beckman Coulter, Brea, CA., USA). The content of thiol groups entrapped within the nanoparticles was determined by the relation between the measuring of non-entrapped thiol groups in the supernatant.

The EE and LE of the CS-GSH nanoparticles were calculated using the following equations:

$$EE\ (\%) = \frac{actual\ amount\ of\ GSH\ entrapped\ in\ NP}{the\ theoretical\ amount\ of\ GSH\ entrapped\ in\ NP} x\ 100$$

$$LE\ (\%) = \frac{actual\ amount\ of\ GSH\ entrapped\ in\ NP}{weight\ of\ NP} x\ 100$$

Preparation of FITC-CS and Rhodamine-CS nanoparticles

LMW chitosan was dissolved in 1% v/v aqueous acetic acid to prepare a 0.3% w/v chitosan solution. Then 1 mL of FITC in methanol (0.5 mg/mL) was added to 20 mL of chitosan solution under stirring. The mixture was stirred for 3 h in the dark at room temperature, then TPP (1:1 v/v) solution was quickly added to the labeled chitosan, the reaction was carried out for 2 hours, and the resulting suspension was centrifuged 42 000 x g, during 1 h to remove free FITC, passed through a 0.22 μm syringe filter aseptically and stored at 4°C. Rhodamine-NP were prepared following the procedure described above, adding 0.5 mg/mL of Rhodamine 123 instead of FITC.

Cell culture

AML-12 cells, derived from mouse liver, were cultured in DMEM (Corning, NY., USA) medium supplemented with 10% FBS (Biowest-BW, MO., USA), 1% penicillin-streptomycin

(Corning, NY., USA), and incubate at culture conditions 95 % O2, 5% CO2,37 °C and propagate until 85% confluence.

Culture treatments

To evaluate the effect of CS-GSH nanoparticles on cells with GSH depletion using BSO; confluent cells were exposed to BSO 20 mM during 18 hours then two amounts of nanoparticles were added [0.12 µmol GSH /g NP (NP1) and 1.2 µmol GSH /g NP (NP2)] for six hours more to complete a 24 hours treatment, in the other hand we have cells exposed to BSO 20 mM, but instead of chitosan-glutathione (CS-GSH) nanoparticles we added NAC 5 mM. Additionally, controls of each treatment were assayed, and negative control, which means cells without treatment.

Confocal microscopy

Uptake of CS nanoparticles was visualized under a confocal laser scanning electron microscope Olympus, FV1000 (Center Valley, PA., USA). AML-12 cells were grown on #1 thickness glass coverslips in 60 x 15-mm Petri dishes with a density of 50 000 cells in 1.5 mL of culture medium. After 24 h, the medium was removed, and the cells were exposed to Rhodamine-NP or FITC-NP for 6 h. The cells were washed twice with PBS before fixation with 4% paraformaldehyde.

FITC-CS NPs were detected at 488/536–624 nm; excitation/ emission. The cell nucleus was stained for nucleic acids with propidium iodide (PI; 1 mM). PI fluorescence was detected at a lower range of 535/617 nm to distinguish the fluorescence contributed by FITC confidently.

FITC- NP were detected at 488/536–624 nm; excitation/ emission. The cell nucleus was stained for nucleic acids with propidium iodide (PI; 1 mM). PI fluorescence was detected at 535 nm/617 nm; ex/em.

Rhodamine-NP was detected at 511/534 nm; excitation/ emission. The cell nuclei were stained for nucleic acids with DAPI 2 mM (4, 6- Diamidino-2-Phenylindole Dihydrochloride), DAPI fluorescence was detected at 385/400–480 nm; excitation/emission. The results are representative of 3 independent experiments conducted on different days.

MTT Assay

The metabolic probe MTT assay tested the viability of cells after treatments. MTT evaluates mitochondrial function by measuring the ability of viable cells to reduce MTT into a blue formazan product. 1×10^4 cells/well were seeded in 24-well plates and exposed as previously described. Hydrogen peroxide was used as positive control. After the exposure, the medium was removed from each well, and cells washed with PSB 1x two times to avoid interference. The resulting formazan product was dissolved in acidified isopropanol. Further, 100 µL was transferred into 96-well plate, and absorbance was measured at 570 nm using a microplate reader.

Intracellular and extracellular thiol content

Total intracellular and extracellular thiol content was determined with Ellman's reagent. After exposure, cells were harvested and homogenized in lysis buffer (0.1% Triton X-100, 100 mM PMSF, 5 mM EDTA in PBS pH 7.4), culture media was employed to determine extracellular glutathione; in both cases, protein interference was avoided by sulfosalicylic acid at 5% protein precipitation and centrifugation at 13,500 g. Supernatants were treated with Ellman's reagent, which reacts with free sulfhydryl groups forming a yellow compound, and this was quantified at 450 nm using a microplate reader.

Total RNA isolation and cDNA synthesis

Cells were cultured in 6-well plates and exposed as the previous description at the end of the treatment; RNA was extracted using TRIzol (Invitrogen, Carlsbad, CA., USA). The concentration of the extracted RNA was determined by absorbance at 240 nm. Purity was estimated by 260/280 and 260/230 ratio. The integrity of RNA was visualized on 1% agarose gel and imagined on a UV transilluminator (Bio-Rad, Hercules CA, USA). One microgram of total RNA was reverse-transcribed to cDNA using M-MLV reverse transcriptase (Invitrogen Carlsbad, CA, USA) and oligo (dT) primers (Promega, Madison, USA) according to the manufacturer's protocol.

The quantitative real-time PCR analysis

Quantitative real-time PCR (qPCR) was performed as follows. Each reaction consists of 5 µL of Kapa SYBR FAST (Kapa Biosystems, Woburn, MA., USA), 3 µL of cDNA, and water to a final volume of 10 µL. Real-time PCR cycle conditions were denaturation 10 min at 95°C followed by 30 cycles of denaturalization at 95°C for 30 sec, annealing at 60°C for 30 sec and elongation at 72°C for 30 sec. The specific primers sequences for each antioxidant genes were the following:

The amplicons were verified by electrophoresis on a 2% agarose gel and visualized on a UV transilluminator. Expressions of selected genes were normalized to beta-actin (ACTB) gene (Table 1), which was used as an internal housekeeping control. All the qPCR experiments were performed by triplicated and data expressed as the mean of at least three independent experiments.

GEN	ACCESSION	SENSE 5' à 3'	ANTISENSE 5'à 3'
ACTB	NM_007393.5	CCAGGTCAT CACTATTGG CAACGAG	TCACACTGC AACTGTTAG GCATTTCT
Nr-f2	NM_010902.4	TACTCCAGG TTGCCACAT T	ACTCAGCGA ACGGGACCT AT
Grx-1	XM_006517477. 1	TGGAGAAAG AGGGAAGAA ATCCTCAGT CA	TATCCGCCT ACGTCACTA GATTAGAGG T

Table 1. Sequences of primers used in qrt-pcr.

Statistical analysis

Each assay was performed in triplicate. We reported the means ± SE, and significance was assessed by a one-way ANOVA, followed by Tukey multiple mean comparison tests as indicated in each case. A P value of <0.05 was considered significant in all cases.

RESULTS AND DISCUSSION

Manufacturing and physicochemical properties of

CS-GSH nanoparticles

CS-GSH nanoparticles were prepared and physicochemical characterized. They were manufactured trough the cross-linking process induced by the electrostatic interactions between chitosan and TPP, resulting in a Polydispersity Index (PDI) less than 0.3, which indicates that a homogeneous dispersion of CS-GSH nanoparticles was obtained. PDI describes the particle size distribution of the nanoparticles, values close to 0 exhibited a homogeneous dispersion, while those greater 0.3 showed high heterogeneity [28]. The Z potential of the chitosan-GSH nanoparticles reflects the density of the surface charge, and it is influenced by the composition of the particles and the medium in which they are dispersed [29]. In aqueous solution, chitosan changes and its conformation become more flexible even with the presence of TPP; the overall surface charge becomes positive in the nanoparticles obtained (64.55mV) (Table 2). The Z potential is higher than ±30 mV, suggesting that the nanoparticles are stable, preventing their aggregation in suspension due to the repulsion of surface charge.

Z Potential	Size	PDI
(mV)	(nm)	
64.55	182.2	0.258

Table 2. Physicochemical properties of cs-gsh nanoparticles.

TEM analysis confirmed the presence of spherical nanoparticles and revealed their morphological properties. TEM images of CS-GSH nanoparticles prepared under the optimized conditions can be observed in (Figure 1). Nanoparticles showed a dense in a structure that ranged from approximately 140 to 290 nm, which is the range of particle size obtained from DLS. Variations can be explained because, in TEM measures, the particles are dried during sample preparation, DLS measures the hydrodynamic particle size.
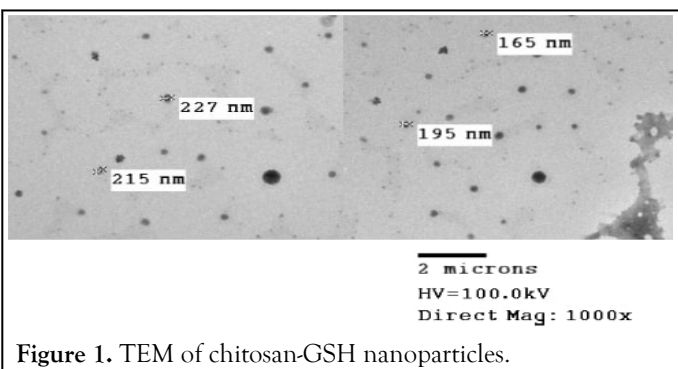
Figure 1. TEM of chitosan-GSH nanoparticles.

Cellular uptake

Confocal microscopy was employed to know the location of the nanoparticles. The results obtained showed nanoparticles in the nuclei after 6 hours of exposure to FITC-NP and Rhodamine-NP (Figures 2 and 3). The presence of both labeled NPs was observed inside the cells. These results suggest that nanoparticles permeate the cellular membrane and enter the cell reaching the nuclei.
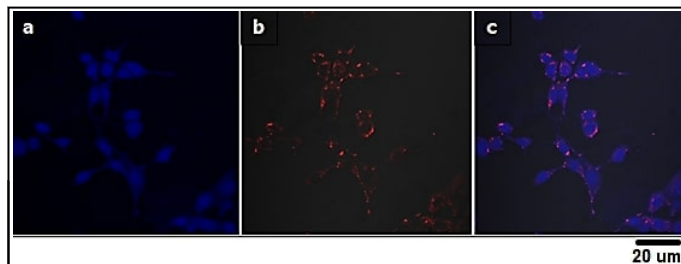
Figure 2. Nanoparticle cellular uptake on AML-12 nuclei cells stained with DAPI and -Rhodamine-NP after 6 h using confocal microscopy. From left to right, cell nuclei stained with DAPI (a), rhodamine fluorescence (b), and the merged image (c). Rhodamine 123-NP are around the nuclei.
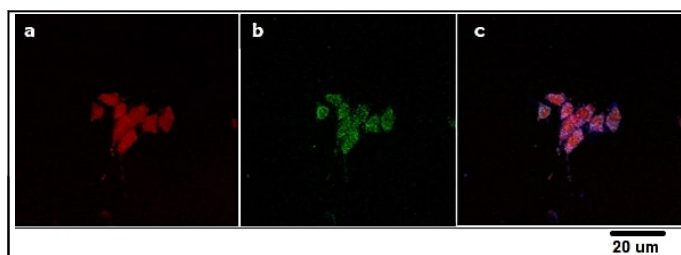
Figure 3. Nanoparticle cellular uptake on AML-12 cells stained with PI, FITC-NP after 6 h using confocal microscopy. From left to right, cell nuclei stained with PI (a), fluorescein fluorescence (b), and the merged image(c). FITC-NP are distributed into the nuclei.

Several studies have established the ability of nanoparticles of chitosan to modulate the permeability of tight junctions in epithelial absorption functions[30–32], increasing the possibility to let particles small enough to go from the nasal cavity or the alveolar sacs into the circulation[31,33]. These properties have been attributed to the positive charges present on its surface[34], which facilitates enter the cells and release molecules of therapeutic interest too. The cationic profile on the surface of these nanoparticles offers the possibility of interaction with glycoproteins and helps nanoparticles enter the cell *via* endocytosis[32].

MTT viability assay

Assessment of AML-12 cell viability was performed using MTT assay, according to the treatment described above. Chitosan-GSH nanoparticles evaluated in two logarithmic concentrations showed dose-dependent effects in the cells. All treatments showed a decrease in cell viability respect to the control except for the BSO with NP2 treatment in which no significant reduction in cell viability was observed (Figure 4). Additionally, reduction in viability was less pronounced in those cells treated with antioxidants such as NAC and CS-GSH nanoparticles;

after treatment with BSO cells treated with NP2 showed a restore cell viability. Like other materials, chitosan in the macroscopic scale is biocompatible and harmless, but chitosan nanoparticles might modify cell viability (Figure 4). There are pieces of evidence about the cytotoxic profiles of chitosan nanoparticles, depending on the properties of the material used in the synthesis, nanoparticle size, the chitosan molecular weight, and cell type [35]. It has been shown that nanoparticles between 110-390 nm prepared with chitosan with molecular weights between 10 kDa -213 kDa and 46%-88% degree of acetylation, showed cytotoxicity profiles in A549 cells [36,37]. When cells were exposed to BSO, viability decreased similarly compared to cultures exposed to H2O2. However, when cells were exposed to BSO and nanoparticles, viability was significantly restored by using the highest dose of nanoparticles (NP2. Naturally, there is a difference between the extra- and intra-cellular redox environments; the glutathione and thiol system is one of the most important cellular antioxidant systems and acts as the primary redox buffer in the cells, it is responsible for the reduced environment [38]. So, an excess of cysteine and thiol leads to an unbalance between the extra- and intra-cellular redox-environments and could bring several effects for cells, which might be related to the decreased cellular viability observed when they were treated with NAC, and those pre-treated with BSO and then with NAC.
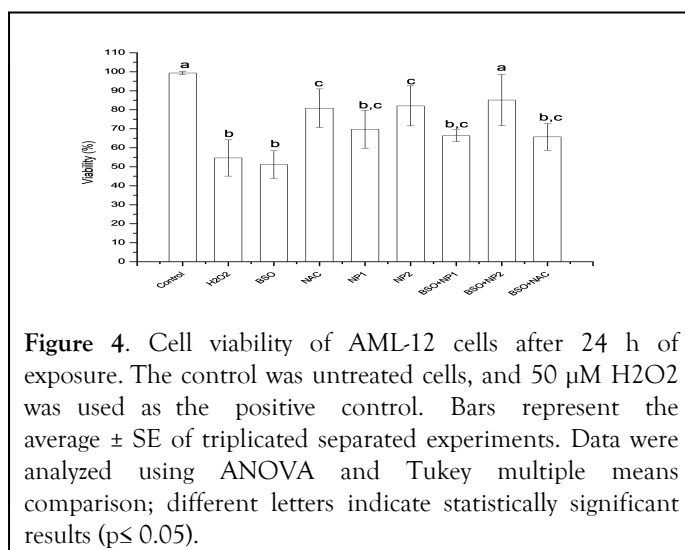
Figure 4. Cell viability of AML-12 cells after 24 h of exposure. The control was untreated cells, and 50 μM H2O2 was used as the positive control. Bars represent the average ± SE of triplicated separated experiments. Data were analyzed using ANOVA and Tukey multiple means comparison; different letters indicate statistically significant results (p≤ 0.05).

Thiol content

The thiol content was determined intra and extracellularly to investigate the effectiveness of CS-GSH nanoparticles to transport GSH into the cells. The results showed higher amount of free thiol on extracellular space than to the intracellular, except for the NP2 treatment, in that case, intracellular thiol was higher than extracellular thiol; another important observation was in the group treated with BSO and NP2 we could notice that intracellular thiol content is significantly higher respect to the control and BSO exposed cultures (Figure 5).
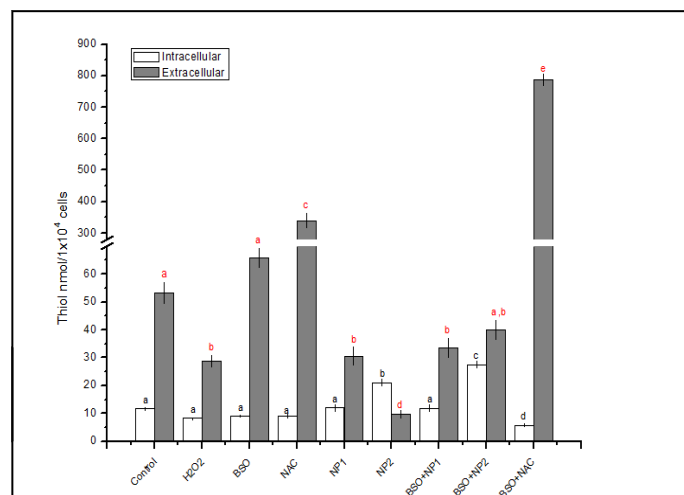
Figure 5. Intracellular thiol content in AML-12 cells (clear bars) after exposure to BSO 20 mM, NAC 5 mM, NP1 and NP2, and extracellular thiol content (dark bars). The values are the average of three separate experiments. Data were analyzed using ANOVA and Tukey multiple mean comparison; different letters indicate statistically significant results, red for extracellular and black for intracellular (p≤ 0.05).

The combined exposure of BSO and NAC shows sensitivity dependent on the thiol response in cells by inhibiting the synthesis of GSH. We observed in the cultures treated with BSO and NAC intracellular thiol values lower than the control cultures. On the other side, NP1 and NP2 moderately restored the thiol content when BSO inhibited the synthesis of GSH in the cultures.

Extracellular thiol content was higher in cells treated with NAC and lower on cells treated with nanoparticles. We could observe that in the cultures treated with NAC, the values of extracellular thiol content were up to 100 nmol/$1x10^5$cells/mL, suggesting that NAC did not enter the cell and stayed in the culture media. NAC is a compound containing a free thiol group which reacts with Ellman's reagent and forms a colorful complex quickly [39].

The basal extracellular thiol content decreases in the cells treated with nanoparticles, suggesting possible thiol transport from the media to the cell by nanoparticles and a redox reaction of thiols.

As we know, GSH is a vital intracellular antioxidant that participates in the removal of reactive species such as hydroxyls, peroxyls, and endogenous and exogenous (from xenobiotics) substrates of P450 enzymes. It acts as a redox buffer in the cells, and it is responsible for the overall highly reduced environment[38]. Cellular regulation of the glutathione system is complex and involves sophisticated signaling networks not entirely understood. Thus, several different signals and mechanisms working alone or together, many signaling ways

increases the complexity and add difficulties to understand redox control and associated processes. In humans, the reduction of cellular GSH levels is associated with oxidative stress diseases and aging [40–42]. GSH is not imported into cells [14]; then, CS-GSH nanoparticles offer the opportunity to introduce GSH into the cells and improve the release of many drugs of therapeutic interest [43,44].

On the other hand, CS-GSH nanoparticles elevated the levels of intracellular thiols without a significant increase in cytotoxicity in a dose-dependent manner, the highest dose of CS-GSH nanoparticles (NP2) was able to improve cell viability after BSO treatment.

Analysis of expression

The Nrf2 and GRx-1 mRNA expression results are plotted in (Figures 6 and 7), respectively. The results showed an increase in Nrf2 expression in cells treated with NP1, suggesting that NAC and the nanoparticles (NP1 and NP2) can enhance or promote Nrf2 expression contrary to BSO treatment; however, BSO triggered mRNA expression of Grx-1; interestingly, a similar effect was also observed in PC12 cells [9]. When the cells were exposed first to BSO, and then with nanoparticles in all cases is observed a relationship between the increase of the gene expression with the amount of CS-GSH nanoparticles and moderately with NAC, although the results were not statistically significant. When the effect of BSO modified the oxide reduction state and then nanoparticles were added to the cultures, the gene response associated with the expression of NRf2 was increased. The combined effect of BSO-NAC in cultures on NRf2 and GRx-1 confirms the cellular sensitivity of this factor concerning to redox modulation.
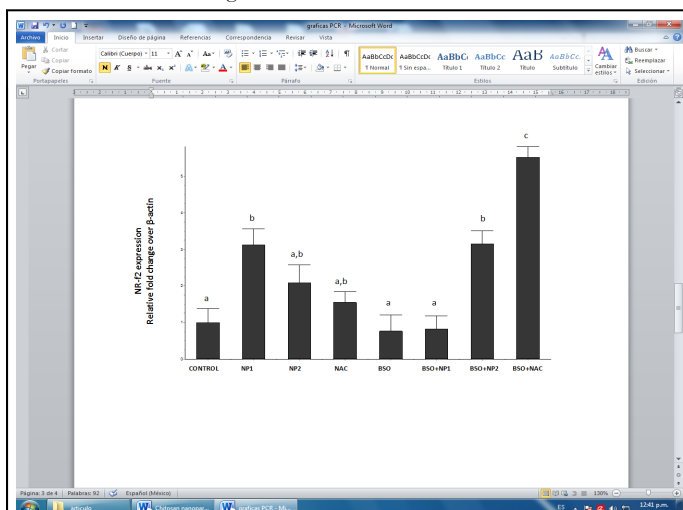
Figure 6. Nrf2 mRNA expression in AML-12 cells after exposure to BSO 20 mM, NAC 5 mM, and CS-GSH

nanoparticles compared with control treatment. Change values were calculated using the 2ΔΔCt method, using the β-actin gene. Values are the average of three independent experiments. Bars represent mean ± SE of triplicated experiments. Data were analyzed using ANOVA and Tukey multiple means comparison; different letters indicate statistically significant results (p≤ 0.05).
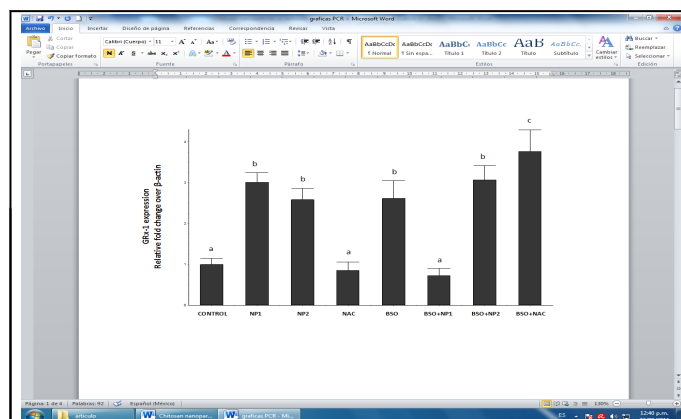
Figure 7. GRx-1 mRNA expression in AML-12 cells after exposure to BSO 20 mM, NAC 5 mM, and CS-GSH nanoparticles compared with control cells. Change values were calculated using the 2ΔΔCt method using the β-actin gene. Values are the average of three independent experiments. Bars represent mean ± SE of triplicated experiments. Data were analyzed using ANOVA and Tukey multiple means comparison. Different letters indicate statistically significant results (p≤ 0.05).

BSO pre-treatment also induces mRNA expression of Nrf2 and Grx-1 in the same way; this may be due to the function of Nrf2, which orchestrates a transcriptional program in response to micro environmental challenges caused by oxidants, electrophiles, and pro-inflammatory agents, allowing adaptation and survival under stress conditions [45]. Nrf2 system regulates the synthesis of a large number of diverse detoxification, antioxidant, and anti-inflammatory molecules, with essential roles in cell metabolism, placing Nrf2 at the interface of redox and intermediary metabolism[45,46]. Redox regulation involves a variety of complex signaling networks where the concentrations of cellular thiols and ROS play a crucial role; although glutathione is stable inside the cell, it can be easily Hydrolyzed by ɣ-L-Glutamyl Transpeptidase (GGT) and Dipeptidase (DP) during export or in the extracellular region so; SH group of glutathione could be conjugate with many different molecules which may include several transcriptional factors involved in redox signaling. In other ways, polymers like chitosan showed positive effects on the expression levels of enzymatic antioxidants enhancing the mRNA expression of SOD-1, GST and reduced the NF-kB activation under H2O2 in a concentration-dependent manner on Chang liver cells and BV-2 cells [47,48].

Deliver GSH systems has pharmacological and clinical importance due redox-sensitivity of the bio-reducible linkers containing thiols because they can be used on the drug delivery system to incorporate and passes from the poorly reducing extra-cellular environments to the actively reducing intra-cellular compartments. This phenomenon has been used for many drug carriers to provide a mechanism of biodegradation. However, successful therapeutic applications should mostly investigate. Concluding, Chitosan-glutathione nanoparticles could enter the cells and counteract the depletion of GSH caused by BSO in AML-2 cells.

 The results showed nanoparticles into the cells and an increase of thiol content where nanoparticles were present, as well as an increase of the expression of Nrf2 and Grx-1in a dose-dependent manner. The results obtained in this work are important and open a broad panorama in the study of the associated redox signaling pathways, where glutathione exerts significant modulating events that can modify various cellular responses associated with cytotoxicity.

ACKNOWLEDGMENTS

REFERENCES

1. Wu WH, Chao CC, Wang FS. Reducing the effects of drug toxicity on glutathione metabolism. J Taiwan Inst Chem Eng. 2016; 60:113-8.

2. Valdovinos-Flores C, Gonsebatt ME. The role of amino acid transporters in GSH synthesis in the blood–brain barrier and central nervous system. Neurochem Int. 2012;61(3):405-14.

3. Ogasawara Y, Takeda Y, Takayama H, Nishimoto S, Ichikawa K, Ueki M, et al. Significance of the rapid increase in GSH levels in the protective response to cadmium exposure through phosphorylated Nrf2 signaling in Jurkat T-cells. Free Radic Biol Med. 2014; 69:58-66.

4. Timme-Laragy AR, Goldstone JV, Imhoff BR, Stegeman JJ, Hahn ME, Hansen JM. Glutathione redox dynamics and expression of glutathione-related genes in the developing embryo. Free Radic Biol Med. 2013;65:89-101.

5. Liu Y, Hyde AS, Simpson MA, Barycki JJ. Emerging regulatory paradigms in glutathione metabolism. Advances in cancer research. 2014;122:69-101.

6. Diaz-Vivancos P, de Simone A, Kiddle G, Foyer CH. Glutathione–linking cell proliferation to oxidative stress. Free Radic Biol Med. 2015;89:1154-64.

7. Lu SC. Glutathione synthesis. Biochim Biophys Acta (BBA)-Gen Subj. 2013;1830:3143-53.

8. Garza-Lombó C, Petrosyan P, Tapia-Rodríguez M, Valdovinos-Flores C, Gonsebatt ME. Systemic L-buthionine-SR-sulfoximine administration modulates glutathione homeostasis via NGF/TrkA and mTOR signaling in the cerebellum. Neurochem Int. 2018;121:8-18.

9. Li H, Wu S, Chen J, Wang B, Shi N. Effect of glutathione depletion on Nrf2/ARE activation by deltamethrin in PC12 Cells. Arh Hig Rada Toksikol. 2013;64(1):87-96.

10. Zhou Y, Wen Z, Zhang J, Chen X, Cui J, Xu W, et al. Exogenous glutathione alleviates salt-induced oxidative stress in tomato seedlings by regulating glutathione metabolism, redox status, and the antioxidant system. Sci Hortic. 2017; 220:90-101.

11. Bilinsky LM, Reed MC, Nijhout HF. The role of skeletal muscle in liver glutathione metabolism during acetaminophen overdose. J Theor Biol. 2015; 376:118-33.

12. Kurahashi T, Lee J, Nabeshima A, Homma T, Kang ES, Saito Y, et al. Ascorbic acid prevents acetaminophen-induced hepatotoxicity in mice by ameliorating glutathione recovery and autophagy. Arch Biochem Biophys. 2016 ;604:36-46.

13. Khayyat A, Tobwala S, Hart M, Ercal N. N-acetylcysteine amide, a promising antidote for acetaminophen toxicity. Toxicol Lett. 2016 ; 241:133-42.

14. Schmitt B, Vicenzi M, Garrel C, Denis FM. Effects of N-acetylcysteine, oral glutathione (GSH) and a novel sublingual form of GSH on oxidative stress markers: A comparative crossover study. Redox Biol. 2015;6:198-205.

15. Koo SH, Lee JS, Kim GH, Lee HG. Preparation, characteristics, and stability of glutathione-loaded nanoparticles. J Agric Food Chem. 2011;59(20):11264-9.

16. Yousefpour P, Atyabi F, Dinarvand R, Vasheghani-Farahani E. Preparation and comparison of chitosan nanoparticles with different degrees of glutathione thiolation. DARU. J Faculty Pharm, Tehran Univ Med Sci. 2011;19(5):367.

17. Kafedjiiski K, Föger F, Werle M, Bernkop-Schnürch A. Synthesis and in vitro evaluation of a novel chitosan–glutathione conjugate. Pharm Res. 2005; 22(9):1480-8.

18. Webber V, de Siqueira Ferreira D, Barreto PL, Weiss-Angeli V, Vanderlinde R. Preparation and characterization of microparticles of β-cyclodextrin/glutathione and chitosan/glutathione obtained by spray-drying. Food Res Int. 2018;105:432-9.

19. Jin X, Xu Y, Shen J, Ping Q, Su Z, You W. Chitosan–glutathione conjugate-coated poly (butyl cyanoacrylate) nanoparticles: Promising carriers for oral thymopentin delivery. Carbohydr polym. 2011 ;86(1): 7.

20. Perrone M, Lopalco A, Lopedota A, Cutrignelli A, Laquintana V, Franco M, et al. S-preactivated thiolated glycol chitosan useful to combine mucoadhesion and drug delivery. Eur J Pharm Biopharm. 2018;132:103-11.

21. Laffleur F, Fischer A, Schmutzler M, Hintzen F, Bernkop-Schnürch A. Evaluation of functional characteristics of preactivated thiolated chitosan as potential therapeutic agent for dry mouth syndrome. Acta Biomater. 2015;21:123-31.

22. Zhang Y, Zhou S, Deng F, Chen X, Wang X, Wang Y, et al. The function and mechanism of preactivated thiomers in triggering epithelial tight junctions opening. Eur J Pharm Biopharm. 2018;133:188-99.

23. Bonengel S, Haupstein S, Perera G, Bernkop-Schnürch A. Thiolated and S-protected hydrophobically modified cross-linked poly (acrylic acid)–a new generation of multifunctional polymers. Eur J Pharm Biopharm. 2014 ;88(2):390-6.

24. Bonengel S, Bernkop-Schnürch A. Thiomers—from bench to market. J Control Release. 2014; 195:120-9.

25. Piña Olmos S, Díaz Torres R, Elbakrawy E, Hughes L, Mckenna J, Hill MA, et al. Combinatorial use of chitosan nanoparticles, reversine, and ionising radiation on breast cancer cells associated with mitosis deregulation. Biomolecules. 2019;9(5):186.

26. Kafedjiiski K, Krauland AH, Hoffer MH, Bernkop-Schnürch A. Synthesis and in vitro evaluation of a novel thiolated chitosan. Biomaterials. 2005;26(7):819-26.

27. Eyer P, Worek F, Kiderlen D, Sinko G, Stuglin A, Simeon-Rudolf V, et al. Molar absorption coefficients for the reduced Ellman reagent: Reassessment. Anal Biochem. 2003; 312(2):224-7.

28. Rampino A, Borgogna M, Blasi P, Bellich B, Cesàro A. Chitosan nanoparticles: Preparation, size evolution and stability. Int J Pharm. 2013;455:219-28.

29. Antoniou J, Liu F, Majeed H, Qi J, Yokoyama W, Zhong F. Physicochemical and morphological properties of size-controlled

chitosan–tripolyphosphate nanoparticles. Colloids Surf A: Physicochem Eng Asp. 2015 ;465:137-46.

30. Lesniak A, Salvati A, Santos-Martinez MJ, Radomski MW, Dawson KA, Åberg C. Nanoparticle adhesion to the cell membrane and its effect on nanoparticle uptake efficiency. J Am Chem Soc. 2013 ;135(4):1438-44.

31. Musumeci T, Pellitteri R, Spatuzza M, Puglisi G. Nose-to-brain delivery: Evaluation of polymeric nanoparticles on olfactory ensheathing cells uptake. J Pharm Sci. 2014;103(2):628-35.

32. Fan W, Yan W, Xu Z, Ni H. Erythrocytes load of low molecular weight chitosan nanoparticles as a potential vascular drug delivery system. Colloids Surf B Biointerfaces. 2012;95:258-65.

33. Fazil M, Md S, Haque S, Kumar M, Baboota S, kaur Sahni J, et al. Development and evaluation of rivastigmine loaded chitosan nanoparticles for brain targeting. European J Pharm Sci. 2012;47(1): 6-15.

34. Abd Elgadir M, Uddin MS, Ferdosh S, Adam A, Chowdhury AJ, Sarker MZ. Impact of chitosan composites and chitosan nanoparticle composites on various drug delivery systems: A review. J Food Drug Anal. 2015;23(4):619-29.

35. Loh JW, Yeoh G, Saunders M, Lim LY. Uptake and cytotoxicity of chitosan nanoparticles in human liver cells. Toxicol Appl Pharmacol. 2010;249(2):148-57.

36. Huang M, Khor E, Lim LY. Uptake and cytotoxicity of chitosan molecules and nanoparticles: effects of molecular weight and degree of deacetylation. Pharm Res. 2004 ;21(2):344-53.

37. Xia W, Liu P, Zhang J, Chen J. Biological activities of chitosan and chitooligosaccharides. Food Hydrocoll. 2011;25(2):170-9.

38. Couto N, Wood J, Barber J. The role of glutathione reductase and related enzymes on cellular redox homoeostasis network. Free Radic Biol Med. 2016;95:27-42.

39. Peng H, Chen W, Cheng Y, Hakuna L, Strongin R, Wang B. Thiol reactive probes and chemosensors. Sensors. 2012;12(11):15907-46.

40. Allocati N, Masulli M, Di Ilio C, Federici L. Glutathione transferases: substrates, inihibitors and pro-drugs in cancer and neurodegenerative diseases. Oncogenesis. 2018;7(1):1-5.

41. Prasad S, Gupta SC, Tyagi AK. Reactive Oxygen Species (ROS) and cancer: Role of antioxidative nutraceuticals. Cancer Lett. 2017;387:95-105.

42. Sindhi V, Gupta V, Sharma K, Bhatnagar S, Kumari R, Dhaka N. Potential applications of antioxidants–A review. J Pharm Res. 2013;7(9):828-35.

43. Brülisauer L, Gauthier MA, Leroux JC. Disulfide-containing parenteral delivery systems and their redox-biological fate. J Control Release. 2014;195:147-54.

44. Leichner C, Jelkmann M, Bernkop-Schnürch A. Thiolated polymers: Bioinspired polymers utilizing one of the most important bridging structures in nature. Adv Drug Deliv Rev. 2019;151:191-221.

45. Hayes JD, Dinkova-Kostova AT. The Nrf2 regulatory network provides an interface between redox and intermediary metabolism. Trends Biochem Sci. 2014;39(4):199-218.

46. Dinkova-Kostova AT, Kostov RV, Canning P. Keap1, the cysteine-based mammalian intracellular sensor for electrophiles and oxidants. Arch Biochem Biophys. 2017;617:84-93.

47. Trinh MD, Ngo DH, Tran DK, Tran QT, Vo TS, Dinh MH, et al. Prevention of H2O2-induced oxidative stress in Chang liver cells by 4-hydroxybenzyl-chitooligomers. Carbohyd Polym. 2014;103:502-9.

48. Oh SH, Vo TS, Ngo DH, Kim SY, Ngo DN, Kim SK. Prevention of H2O2-induced oxidative stress in murine microglial BV-2 cells by chitin-oligomers. Process Biochem. 2016;51(12):2170-5.